

Stress Prediction in the Dynamic Compression Plate with Changing the Configuration of the Screw Fixation

Boonthum Wongchai

Department of Mechanical Engineering, Faculty of Engineering at Si Racha,
Kasetsart University, 199 M.6, Tungsukhla, Si Racha, Chonburi, 20230, Thailand

Abstract: Problem statement: Human femur fracture is one of the most frequent type of bone fractures. One of the widely used methods in an internal fixation is an application of the Dynamic Compression Plate (DCP). The configuration of the screw fixation plays a major role of the DCP stress. **Approach:** This research is proposed to investigate the stress distribution in the 14-hole DCP by using Finite Element Analysis (FEA), eight configurations of the screw fixation with the body weight of 50 and 70 kg. The maximum von Mises stress on the DCP in each configuration is used to find the best of the screw fixations. The equations of the maximum von Mises stress are formulated by the regression analysis. **Results:** The experimental results show that the relation of the maximum von Mises stress and the number of screws are the linear equation. **Conclusion:** The maximum von Mises stress from FEA could be predicted by using the linear equation.

Key words: Stress prediction, screw fixation, dynamic compression plate, femur fracture

INTRODUCTION

Femur fracture is the most significant osteoporotic fracture. The Dynamic Compression Plate (DCP) is one of the most commonly used implants for internal fixation. The body load will be transmitted from the screw through the DCP. The DCP fails when the maximum von Mises stress is greater than the yield strength of DCP material. The internal fixation devices are usually made of non-corrosive metal such as stainless steel and titanium alloys. Nowadays the fiber reinforce composite materials have been investigated for the new choices better than stainless steel and titanium alloys (Kim *et al.*, 2010). The cyclic body load is an important force during walking varies from 0 to full body load. It may cause the plate is damaged by fatigue mode (Kanchanomai *et al.*, 2008; Ahmad *et al.*, 2007).

When the fracture occurs at the middle part of the femur, the physician will cut the fracture and form a gap of 1 to 10 mm. Subsequently, the fractured femur is bridged by using an internal fixation plate. The interfragmentary strain (IFS) is defined as the ratio of the fracture gap displacement after the body load applied and the original fracture gap. The best IFS range between 2% to 10% (Perren, 1979). The fracture gap about 1 to 10 mm usually used in the research (Kim *et al.*, 2010; Kanchanomai *et al.*, 2008; Ahmad *et al.*, 2007; Stoffel *et al.*, 2003; Saffar *et al.*, 2009; Sadi *et al.*, 2010).

There are many causes affecting the DCP stress, including the DCP length, number of holes, the screw preload, the fracture gap, the configuration of the screw

fixation and etc. The configuration of the screw fixation plays a major role of the DCP stress.

MATERIALS AND METHODS

Finite Element Analysis (FEA): The three-dimension finite element model is modeled from the second generation femur of Pacific Research Lab (Vieccenti *et al.*, 2003). Each screw configuration is modeled in SolidWorks 2004 software and transformed into finite element models by using ABAQUS 6.4 software with the four-node tetrahedral elements.

The DCP and the screw material are 316L stainless steel, with Young's modulus of 193 MPa and a Poisson's Ratio of 0.3. The femur was composed of the cortical bone and the cancellous bone. The cortical bone is modeled with Young's modulus of 15 GPa and Poisson's Ratio of 0.33, while the cancellous bone is modeled with Young's modulus of 1.1 GPa and Poisson's Ratio of 0.33 (Lengsfeld *et al.*, 1998).

Force Analysis: The ilium shown in Fig.1 is loaded by a half of body load (F_w), the abduction force (F_a) and the hip force (F_h). The force vector polygon is represented in Fig. 2.

The related equations including those mentioned forces are formulated by using the Newton's first law. The summing of the force vectors will be equal to zero.

$$\vec{F}_h + \vec{F}_a + \vec{F}_w = 0 \quad (1)$$

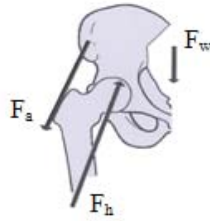


Fig. 1: The body load and the forces on the ilium (Hall 2007)

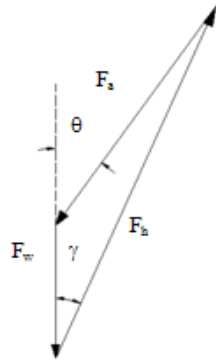


Fig. 2: The force vector polygon

Table 1: Force components in x and y directions

Body weight (kg)	F _{ax} (N)	F _{ay} (N)	F _{hx} (N)	F _{hy} (N)
50	295.56	354.24	-342.36	-592.98
70	413.79	493.13	-479.30	-830.17

Table 2: The screw configurations on each side

Model	Fixed at hole-number	Number of screws
1	1 2 3 4 5 6	6
2	1 3 4 5 6	5
3	1 4 5 6	4
4	1 5 6	3
5	1 6	2
6	1 2 6	3
7	1 2 3 6	4
8	1 2 3 4 6	5

Table 3: The groups of screw configuration

Group	Model	Number of screws
1	5 4 3 2 1	2 3 4 5 6
2	5 6 7 8 1	2 3 4 5 6

From Fig. 2 the values of angle θ and γ were 29° and 19° according to Waide research (Waide *et al.*, 2003). The y axis is aligned along the axial direction of the femur as show in Fig. 3. The forces in x and y directions are

$$F_{ax} = F_a \sin 40^\circ \quad (2)$$

$$F_{ay} = F_a \cos 40^\circ \quad (3)$$

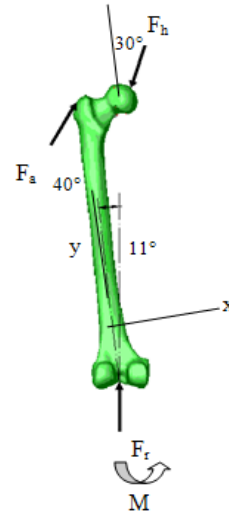


Fig. 3: The free body diagram of the femur

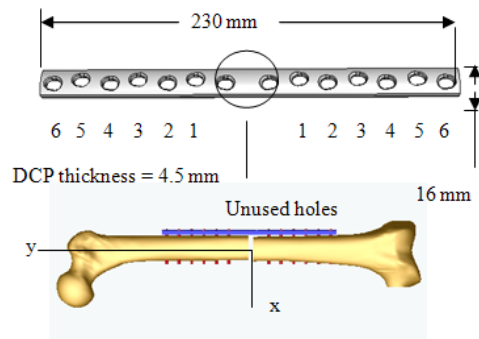


Fig. 4: The hole-number of the DCP

$$F_{hx} = -F_h \sin 30^\circ \quad (4)$$

$$F_{hy} = -F_h \cos 30^\circ \quad (5)$$

From equations (2) to (5) the values of F_{ax} , F_{ay} , F_{hx} and F_{hy} as shown in Table 1, we obtain the body weights of 50 kg and 70 kg.

The forces acting on the femur as shown in Fig. 3 have the opposite directions to their reaction forces in Fig. 1. The angle between y axis and the vertical axis is 11° (Cristofolini *et al.*, 1996; Hall, 2007; Waide *et al.*, 2003). The reaction force (F_r) and the reaction moment (M) occur at the femur and the tibia joint. At this joint, the fixed condition is defined in finite element model.

The screw configurations: The 10-mm fracture gab was bridged by the 14-hole DCP as shown in Fig. 4. The femur and the DCP are fixed by the 4.5-mm

diameter screws. Two screws were fixed at 1st and 6th holes on both sides. The other holes are fixed with additional screws. Two holes at the middle are left without any screws.

The eight configurations of screw fixation are shown in Table 2. The contact conditions are applied on the finite element model, the glue condition between screw and plate, the glue condition between screw and femur and the touching condition between plate and femur.

Two groups of screw configuration are conducted by using the direction of the screw fixation as shown in Table 3. The number of screws varies from 2 to 6.

RESULTS

The results from FEA are shown in Table 4. We found that the maximum von Mises stress on the DCP is occurred in the DCP hole near the fracture gab (unused hole) for all cases as shown in Fig. 5.

From the groups of the screw configuration in Table 3 and the maximum von Mises stress in Table 4, we represented the maximum von Mises stress versus the number of the screws in Fig. 6.

Table 4: The maximum von Mises stress (σ_{von}) on the DCP

Model	Body weight 50 kg	Body weight 70 kg
	σ_{von} (MPa)	σ_{von} (MPa)
1	661	776
2	943	1547
3	947	1459
4	998	1692
5	1203	1991
6	969	1554
7	1026	1507
8	1033	1485

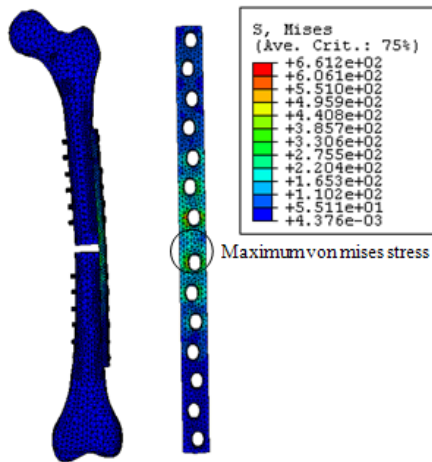


Fig. 5: The von Mises stress on the DCP, body weight 50 kg, model 1

From the regression analysis, we found that the relation of the maximum von Mises stress and the number of screws are the linear equation as follow:

$$\sigma_{von} = a + bN \tag{6}$$

When a and b are constants, while N is number of screws.

The R square (R^2), the statistical significance (α) and the values of a and b, are shown in Table 5.

From equation (6) and Table 5, we could be constructed the linear equations by using the linear regression analysis as shown in Fig. 7-10.

Table 5: The regression analysis and the parameter estimates

Graph	R^2	a	a	b
50 kg group 1	0.865	0.022	1.405×10^3	-113.8
50 kg group 2	0.842	0.028	1.437×10^3	-114.7
70 kg group 1	0.823	0.033	2.523×10^3	-257.5
70 kg group 2	0.732	0.064	2.407×10^3	-236.1

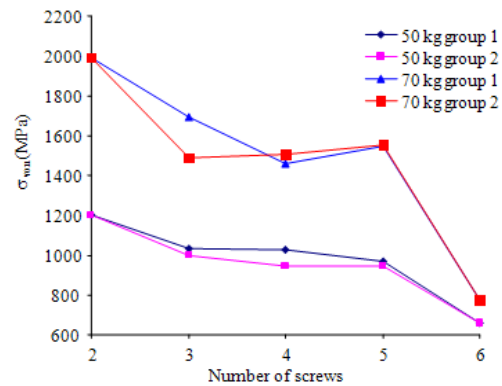


Fig. 6: The maximum von Mises stress versus the number of screws

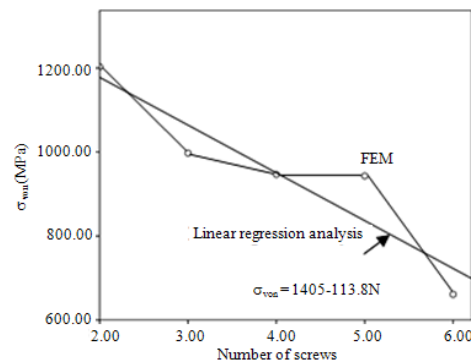


Fig. 7: The linear regression analysis (50 kg group 1)

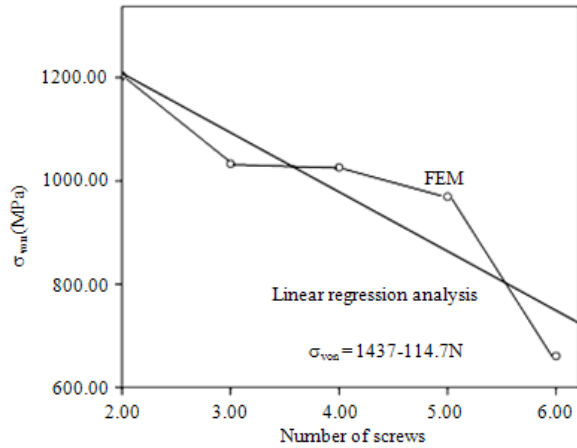


Fig. 8: The linear regression analysis (50 kg group 2)

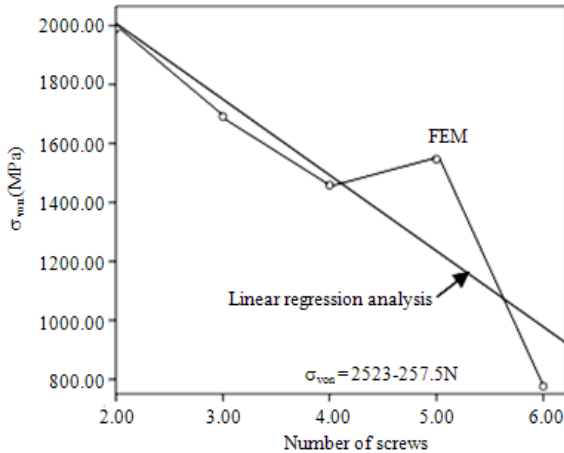


Fig. 9: The linear regression analysis (70 kg group 1)

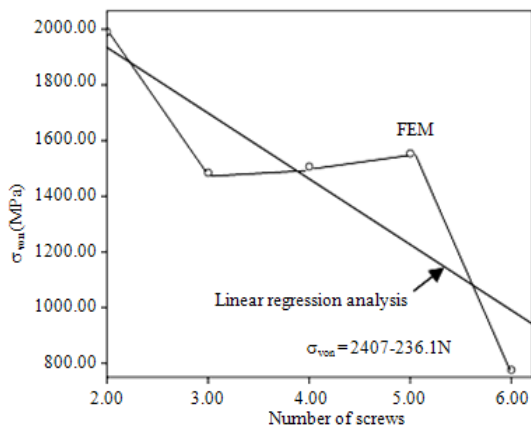


Fig. 10: The linear regression analysis (70 kg group 2)

DISCUSSION

The results from FEA show that the maximum von Mises stress on the DCP occurs in the unused holes for all cases.

From the graph in Fig. 6, it has been found that the relations between the von Mises stress and the number of screws are the inverse variations. The von Mises stress could be decreased by increasing the number of screws. The best of screw configuration is model 1 with six screws on each side.

From the regression analysis in Table 5 and equation (6), we could predict the maximum von Mises stress by using the linear equation with the statistical significance α less than 0.064.

CONCLUSION

The maximum von Mises stress from FEA could be predicted by using the linear equation. We could decrease the maximum von Mises stress on the DCP by adding the number of screw with the groups of screw configuration.

REFERENCES

- Ahmad, M., R. Nanda, A.S. Bajwa, J. Candi-Couto and S. Green *et al.*, 2007. Biomechanical testing of the locking compression plate: When does the distance between bone and implant significantly reduce construct stability? *Injury*, 38, 358-364. PMID: 17296199
- Cristofolini, L., M. Viceconti, A. Cappello and A. Toni. 1996. Mechanical validation of whole bone composite femur models. *J. Biomech.*, 29: 525-535. DOI: 10.1016/0021-9290(95)00084-4
- Hall, S.J., 2007. *Basic Biomechanics*. 5th Edn., McGraw-Hill, New Delhi, ISBN-10: 0071104313, pp: 544.
- Kanchanomai, C., V. Phiphobmongkol and P. Muanjn, 2008. Fatigue failure of an orthopedic implant – a locking compression plate. *Eng. Failure Anal.*, 15: 521-530. DOI: 10.1016/j.engfailanal.2007.04.001
- Kim, S.H., S.H. Chang and H.J. Jung, 2010. The finite element analysis of a fractured tibia applied by composite bone plates considering contact conditions and time-varying properties of curing tissues, *Composite Struc.*, 92: 2109-2118. DOI: 10.1016/j.compstruct.2009.09.051
- Lengsfeld, M., J. Schmitt, P. Alter, J. Kaminsky and R. Leppek, 1998. Comparison of geometry-based and CT voxel-based finite element modelling and experimental validation. *Med. Eng. Phy.*, 20: 515-522. PMID: 9832027

- Perren, SM., 1979. Physical and biological aspects of fracture healing with special reference to internal fixation. *Clin. Orthop. Relat. Res.*, 138: 175-196. PMID: 376198
- Sadi, F., A. Veshkini, D. Sharifi and M.N. Masouleh, 2010. Ultrasonography and radiography evaluation of the cartilage graft in repair of experimentally induced radial bone defect in rabbit. *Am. J. Anim. Vet. Sci.*, 5: 40-44. DOI: 10.3844/ajavsp.2010.40.44
- Saffar, K.P., N. JamilPour and S.M. Rajaai, 2009. How does the bone shaft geometry affect its bending properties? *Am. J. Applied Sci.*, 6: 463-470. DOI: 10.3844/ajassp.2009.463.470
- Stoffel, K., U. Dieter, G. Stachowiak, A. Gachter and M.S. Kuster, 2003. Biomechanical Testing of the LCP- how can stability in locked internal fixators be controlled. *Injury*, 34: 11-19. DOI: 10.1016/j.injury.2003.09.021
- Waide, V., L. Critofolimi, J. Stolk, N. Verdonshot and A. Toni, 2003. Experimental investigation of bone remodelling using composite femurs. *Clin. Biomech.*, 18: 523-536. DOI: 10.1016/S0268-0033(03)00072-X